A Universal Approach to Preparation of Colloidal Mesoporous Platinum Nanoparticles with Controlled Particle Size in a Wide Range from 20 nm to 200 nm

Journal:	*Physical Chemistry Chemical Physics*
Manuscript ID:	CP-COM-01-2014-000039.R1
Article Type:	Communication
Date Submitted by the Author:	08-Mar-2014
Complete List of Authors:	Cuiling, Li; National Institute for Materials Science, WPI Center for MANA Imura, Masataka; National Institute for Materials Science, WPI Center for MANA Yamauchi, Yusuke; National Institute for Materials Science, WPI Center for MANA

PCCP

COMMUNICATION

Cite this: DOI: 10.1039/x0xx00000x

Received 00th January 2012,
Accepted 00th January 2012

DOI: 10.1039/x0xx00000x

A Universal Approach to Preparation of Colloidal Mesoporous Platinum Nanoparticles with Controlled Particle Size in a Wide Range from 20 nm to 200 nm

Cuiling Li,[a] Masataka Imura,[a] and Yusuke Yamauchi[a,b,c]*

a World Premier International (WPI) Research Center for Materials Nanoarchitectonics (MANA), National Institute for Materials Science (NIMS), 1-1 Namiki, Tsukuba, Ibaraki 305-0044, Japan.
b Department of Nanoscience and Nanoengineering, Faculty of Science and Engineering, Waseda University, 3-4-1 Okubo, Shinjuku, Tokyo 169-8555, Japan.
c Precursory Research for Embryonic Science and Technology (PRESTO), Japan Science and Technology Agency (JST), 4-1-8 Honcho, Kawaguchi, Saitama 332-0012, Japan.
E-mail: Yamauchi.Yusuke@nims.go.jp; Homepage: http://www.yamauchi-labo.com

We report a universal method for preparation of mesoporous Pt nanoparticles (MPNs) with tunable particle sizes. MPNs with various particle sizes are simply prepared by changing the surfactant concentration in the starting solutions. Small-sized MPNs show the highest electrochemically surface area and highest current density in methanol oxidation reaction.

Currently, precisely controlled synthesis of Pt nanostructures with tailored shapes and sizes has attracted considerable interest, due to their important role in catalytic applications[1-10], such as methanol/ethanol oxidation reaction, oxygen reduction reaction, and hydrogen/oxygen evolution reaction. The size and shape of Pt nanostructures have a distinct influence on accessibility of catalytically active sites, which can help to improve electrochemical performance and/or enhance mass transportation.

Introduction of mesoporous structures is one of promising strategies to improve surface area and reactivity. Their unique concave surface relative to convex surface of normal Pt nanoparticles.[2-3] Many efforts have been made in the design and synthesis of mesoporous Pt. Several synthetic methods have been developed, including hard-templating approach,[4] surfactant-assisted approach,[5] lyotropic liquid crystal (LLC) approach,[3,6] dealloying approach,[7] and galvanic replacement approach.[8] As the mostly utilized soft-templating way, there are two approaches; (i) LLC approach[3,6] and (ii) micelle assembly approach[9]. Between two methods, there is large difference in the used surfactant concentration. Generally, LLCs are formed, when the surfactant concentration is higher than 30-40 wt%.[3,6] In contrast, in the micelle assembly approach, the surfactant concentration is very low (a few wt%) over critical micelle concentration (CMC).[9] Till now, both methods have demonstrated their own merits in different ways.

In this work, we focus on the effect of the surfactant concentration in the wide range on the particle shapes and sizes in the final products. To the best of our knowledge, there are no reports on the preparation of mesoporous Pt nanoparticles (MPNs) with tunable particle sizes. In the previous studies, various kinds of dendritic Pt and Pt-based alloys have been well obtained by external effect of sonication treatment[10] and heat treatment with/without magnetic stirring.[11] Compared to these previous methods, our approach is quite simple without any complicated steps and facilities. Our previous work demonstrated that the initial Pt concentration played an important key role for the synthesis of dendritic Pt nanoparticles.[12] However, we failed to control their particle sizes. Our target in this study is to develop a universal way to prepare MPNs with controlled particle sizes. Considering practical uses, a large-scale fabrication in an extremely facile way is highly desired.

To prepare MPNs, aqueous solutions consisting of nonionic Brij58 surfactant at various concentrations were firstly prepared under stirring until stable micelle solutions were formed. Then, certain amount of K_2PtCl_4 and ascorbic acid (AA) were added to the surfactant solutions, making the final concentration of K_2PtCl_4 and AA to be 5 mM and 12.5 mM. The final concentration of Brij58 in each solution was varied from 0.01 % to 0.5 %, 1.0 %, 5.0 %, 10.0 %, 15.0 %, and 20.0 %, respectively. Then, all the reaction solutions were incubated without any external treatment for 12 hours at room temperature. After centrifugation at 14,000 rpm with ethanol and water for several times, the black precipitates were collected and for further characterization. The obtained MPNs prepared at various surfactant concentrations were denoted as MPN1 (for 0.01 %),

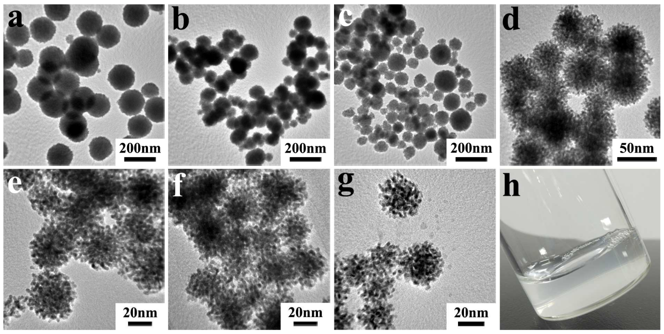

Figure 1 Typical TEM images of a) MPN1, b) MPN2, c) MPN3, d) MPN4, e) MPN5, f) MPN6, and g) MPN7 obtained at 0.01 wt%, 0.5 wt%, 1.0 wt%, 5.0 wt%, 10.0 wt%, 15.0 wt%, and 20.0 wt% Brij58, respectively. h) Photograph of Brij58 solution at the concentration of 30.0 wt%.

MPN2 (for 0.5 %), MPN3 (for 1.0 %), MPN4 (5.0 %), MPN5 (10.0 %), MPN6 (15.0 %), and MPN7 (20.0 %).

Brij58, one of typical nonionic surfactants, was used in this work. For precisely controlling the particle sizes, the concentrations of Brij58 were widely changed in the range of 0.01 wt% to 20.0 wt% and all the concentrations are higher than the CMC ($\mathrm{CMC_{Brij58}}$=0.009 wt%) and lower than the critical concentration for LLC formation. **Figure 1a-g** displayed the typical TEM images of the representative MPNs prepared with 0.01, 0.5, 1.0, 5.0, 10.0, 15.0, and 20.0 wt% of Brij58, respectively. Notable decrease in the particle sizes with increasing the concentrations of Brij58 could be well observed. When the surfactant concentration was higher than 30 wt%, the solution viscosity was drastically increased and then LLCs were formed.

Figure 2b shows wide-angle XRD profiles of the obtained MPNs. Several peaks were assignable to (111), (200), (220), (311), and (222) of Pt *fcc* crystal. The peaks were wider and wider, when more Brij58 was used in the reaction system. The average sizes of single Pt crystals calculated from the Schrrer equation using the strongest diffraction peak of (111) plane were 170 nm (for 0.01 wt%), 90 nm (for 0.5 wt%), 68 nm (for 1.0 wt%), 55 nm (for 5.0 wt%), 40 nm (for 10.0 wt%), 30 nm (for 15.0 wt%), and 26 nm (for 20.0 wt%), respectively. As seen in **Figure 1a-c**, when the particle sizes were large, the internal mesostructures of particles could not be clearly confirmed by TEM observation, because the electron beam cannot pass through the whole particles. To fully investigate the details, all the samples were measured by low-angle XRD (**Figure 2a**). One broad peak was observed at around 1.3° (d = 6.8 nm), indicating the mesostructural periodicity in the particles (*i.e.*, well-organized mesoporous structures). The surface structures of the obtained MPNs were also studied by high-angle annular dark-field scanning TEM (HAADF-STEM). Mesoporous structures could be well observed for each sample. From **Figure S1**, mesopores could be well seen on the whole area, although small particles with ill-growth were also observed. It is proved that mesoporous structures were formed all over the particles, from the most inner part to the outer surface.

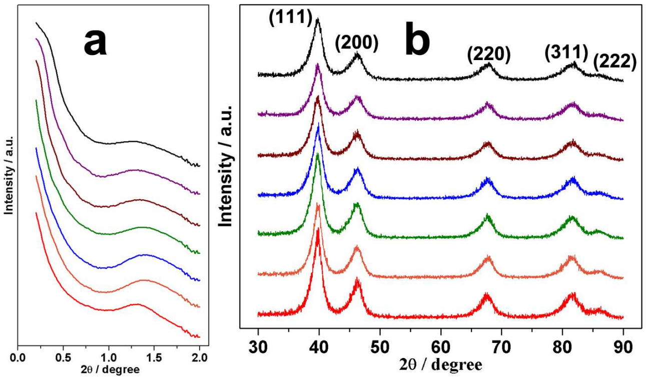

Figure 2 a) Low-angle and b) wide-angle X-ray diffraction (XRD) profiles of MPNs obtained at various Brij58 concentrations. From bottom to top: MPN1, MPN2, MPN3, MPN4, MPN5, MPN6, and MPN7, prepared with 0.01 wt%, 0.5 wt%, 1.0 wt%, 5.0 wt%, 10.0 wt%, 15.0 wt%, and 20.0 wt% Brij58, respectively.

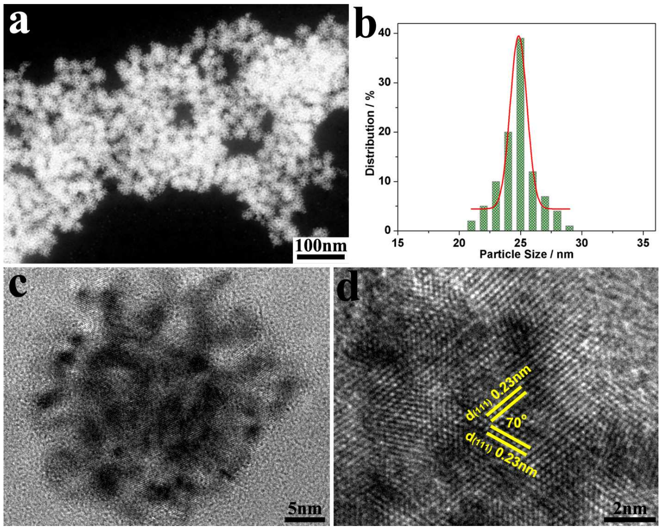

Figure 3 a) High-angle annular dark-field scanning TEM (HAADF-STEM) image, b) Particle size distribution, c) High-magnified bright-field TEM image of one particle, and d) crystalline lattice fringes observed on the particle edge for MPN7 prepared with 20.0 wt% Brij58.

In the present system, Brij58 surfactant concentration is over the CMC, so the surfactants are self-assembled to form the spherical micelles with the hydrophobic parts in the interior and the hydrophilic groups of -CH_2CH_2O- in the exterior. The dissolved Pt species are through to interact on the surface of the micelles.[9] The spherical micelles can serve as the template for the formation of mesopores. As a control experimental, we reduced the Pt species under the same condition without Brij58. Any porous structures were not observed (not shown). Similar phenomena have been confirmed in our previous works.[9] According to low-angle XRD profile (**Figure 2a**), it was proved that all the samples possessed almost the same mesostructural periodicity in the particles.

As seen in **Figures 1** and **S2**, the particle sizes were gradually decreased with the increase of the concentration of Brij58. When the surfactant concentrations gradually increase, the viscosity of

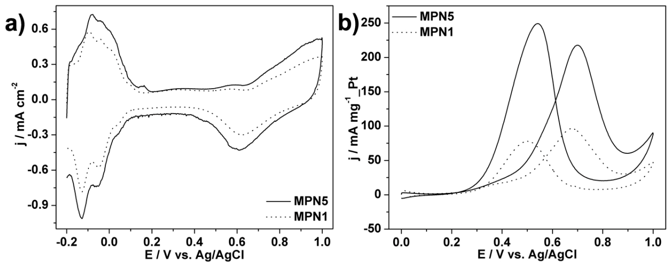

Figure 4 a) Cyclic voltammetry (CV) curves for MPN1 and MPN5 recorded at room temperature in 0.5 M H_2SO_4 solution at a sweep rate of 50 mV· s^{-1}. b) CV curves of MOR catalyzed by MPN1 and MPN5, respectively, in 0.5 M H_2SO_4 solution containing 500 mM methanol at a sweep rate of 50 mV· s^{-1}. The current densities (Y axis) are normalized by the mass of Pt (mg).

solutions becomes high. In the highly concentrated surfactant solution, the dissolved Pt species cannot be diffused easily during the Pt deposition process, due to the high viscosity. Without the surfactants, the Pt species easily moved to the Pt nuclei which are firstly deposited and are reduced on them, that is, the grain growth reaction is preferably occurred. In this case, the particle sizes become relatively large. In contrast, in the presence of highly concentrated surfactant, the Pt species are thought to be deposited without large movement in the surfactant solution. Then, the grain growth reaction would be prevented, thereby decreasing the particle sizes in the products. Similar techniques have been often seen in previous researches in which fine metal nanoparticles are prepared inside polymer hydrogel.[13] In our system, by drastically changing the surfactant concentrations, the particle sizes can be tuned in a wide range from 20 nm to 200 nm, as shown in **Figures 1** and **S2**.

The detailed structures of MPNs obtained at 20.0 wt% Brij58 were further characterized. The image obtained at low magnification (**Figure 3a**) indicated that the as-synthesized product showed well-dispersed nanoparticles with complete porous structures, demonstrating the high-yield formation of the MPNs (100%). The size of the MPNs ranged narrowly from 21 to 29 nm with a dominating diameter of around 25 nm (**Figure 3b-c**). This average particle size is almost equal to the average Pt crystalline size calculated from the Schrrer equation, meaning each particle possesses almost single crystalline nature. Actually, from high resolution TEM image (**Figure S3**), the lattice fringes were coherently extended over the whole particle, although some distortion was observed. As shown in **Figure 3d**, The observed *d* spacing of 0.23 nm between the adjacent fringes and the dihedral angle of 70° corresponded to the (111) diffraction planes of face-centered cubic (*fcc*) structured Pt.

Owing to their highly porous structures, the as-synthesized MPNs surely possess a high surface area, and thus are expected to demonstrate high catalytic performance in electrochemical application. Cyclic voltammetry (CV) was used to evaluate the electrochemical surface areas (ECSAs) of all the MPNs. The ECSAs can provide important information regarding the number of electrochemically available active sites. The higher ECSA surely indicates more electrochemical active sites, revealing the effect of the particle sizes toward the electrochemical performance. Before the CV measurements, the obtained MPNs were subjected to consecutive washing/centrifugation cycles with ethanol to remove the extra surfactants entrapped in the pores of nanoparticles.

Figure 4a compares the CV curves on two typical MPNs (MPN1 and MPN5 were obtained at 0.01 wt% and 10.0 wt% Brij58, respectively) recorded in 0.5 M H_2SO_4 solution at a sweep rate of 50 mV·s^{-1}. The ECSA was calculated by integrating the charge passed in the hydrogen adsorption/desorption region after double-layer correction and assuming that the charge required to oxidize a monolayer of hydrogen on Pt is of 0.21 mC·cm^{-2}. As we expected, the ECSAs of our MPNs showed clearly enhancement with the decrease of the particle sizes (*i.e.*, with increase of the Brij58 concentration), as shown in **Table 1**. By decreasing the particle sizes, the electrolyte can access to the whole pore surface, even the inner pore surface of the particles. The highly accessible surface of the MPNs is expected to realize enhanced electrocatalytic activity.

We evaluated the electrocatalytic performance of the MPNs for methanol oxidation reaction (MOR). The MOR measurement was performed in 0.5 M H_2SO_4 containing 0.5 M methanol by using MPNs-modified glassy-carbon electrode as a working electrode at room temperature with a sweep rate of 50 mV·s^{-1}. **Figure 4b** shows the CV curves of MOR for MPN1 and MPN5 catalysts, respectively. Two obvious anodic peaks, which are typical features of the methanol oxidation process, were observed on both the samples

Table 1 Summary of the ECSA and the MOR performance of the as-prepared MPNs.

Items Sample^a	ECSA(m^2 g^{-1}_Pt)^b	MOR			
		Onset Potential (V)	Peak Potential (V)	Peak Current (mA mg^{-1}_Pt)	Retentivity (%)^c
MPN1	19.7	0.20	0.68	96.6	124.8
MPN2	25.3	0.18	0.69	119.8	102.2
MPN3	30.2	0.21	0.71	131.3	92.9
MPN4	36.7	0.19	0.72	152.8	91.7
MPN5	42.5	0.19	0.70	216.9	92.8
MPN6	48.1	0.19	0.68	228.0	93.5
MPN7	50.3	0.22	0.69	271.7	95.3

^{a}: The MPNs obtained at 0.01, 0.5, 1.0, 5.0, 10.0, 15.0, and 20.0 wt% Brij58 were denoted as MPN1, MPN2, MPN3, MPN4, MPN5, MPN6, and MPN7, respectively;

^{b}: The electrochemical surface area (ECSA) was calculated from the hydrogen adsorption/desorption region of the CV curves obtained after activation;

^{c}: Retentivity means how much the activity could be retained after the chronoamperometric tests at 0.6 V for 2000 s in 0.5 M H_2SO_4 containing 500 mM methanol.

during the positive and negative sweep in the CVs. Onset potentials, peak potentials, and peak currents are important parameters for evaluation of the catalytic performance, as summarized in **Table 1**. All the MPNs have the similar onset potential of ~0.20 V and peak potential of ~0.70 V, indicating all of our MPNs showed similar facility on catalyzing the methanol oxidation. Noticeable difference in the peak current confirmed the different activity of MPNs with various particle sizes. Considering the increasing activity of MPNs with increasing their ECSAs and decreasing the particle sizes, the enhanced catalytic activity might be ascribed to sufficient active sites and excellent permeability in mass transportation. As the structure characterization revealed, the MPNs obtained at highly concentrated Brij58 possessed smaller particles, which is important merit for increasing the electrocatalytic activities. Furthermore, the stability toward MOR for our MPNs was evaluated. The CV curves for MOR were recorded after chronoamperometric tests at 0.6 V for 3000 s in 0.5 M H_2SO_4 solution containing 500 mM methanol. The MPNs could well retain more than 92% of their initial activity, as summarized in **Table 1**.

In summary, we proposed a universal approach for high-yield synthesis of MPNs using Brij58 as surfactant in aqueous solution at room temperature without any external treatment. The present method for the preparation of MPNs is a facile method which shows important merits for large-scale fabrication in industry. The obtained MPNs exhibited enhanced ECSAs and much enhanced catalytic activity for MOR, when the particle size became smaller. The results reported herein suggest that superior catalysts can be developed by controlling the particle sizes.

References

[1] (a) Tian, N.; Zhou, Z.-Y.; Sun, S.-G.; Ding, Y.; Wang, Z. L. Science 2007, 316, 732-735; (b) Xia, B. Y.; Wu, H. B.; Yan, Y.; Lou, X. W.; Wang, X. J. Am. Chem. Soc. 2013, 135, 9480-9485; (c) Wang, L.; Imura, M.; Yamauchi, Y. ACS Appl. Mater. Interfaces 2012, 4, 2865-2869; (d) Stamenkovic, V. R.; Fowler, B.; Mun, B. S.; Wang, G.; Ross, P. N.; Lucas, C. A.; Markovic, N. M. Science 2007, 315, 493-497; (e) Bing, Y.; Liu, H.; Zhang, L.; Ghosh, D.; Zhang, J. Chem. Soc. Rev. 2010, 39, 2184-2202; (f) Liang, H. W.; Cao, X.; Zhou, F.; Cui, C.-H.; Zhang, W.-J.; Yu, S.-H. Adv. Mater. 2011, 23, 1467-1471; (g) Dasgupta, N. P.; Liu, C.; Andrews, S.; Prinz, F. B.; Yang, P. J. Am. Chem. Soc. 2013, 135, 12932-12935; (h) Neyerlin, K. C.; Gu, W.; Jorne, J.; Gasteiger, H. A. J. Electrochem. Soc. 2007, 154, B631-B635; (i) Esposito, D. V.; Hunt, S. T.; Stottlemyer, A. L.; Dobson, K. D.; McCandless, B. E.; Birkmire, R. W.; Chen, J. G. Angew. Chem. Int. Ed. 2010, 49, 9859-9862; (j) Wang, C.; Daimon, H.; Onodera, T.; Koda, T.; Sun, S. Angew. Chem. Int. Ed. 2008, 47, 3588-3591; (k) Giovanni M.; Poh, H. L.; Ambrosi, A.; Zhao, G.; Sofer, Z.; Šaněk, F.; Khezri, B; Webstera, R. D.; Pumera, M. Nanoscale, 2012, 4, 5002-5008.

[2] Warren, S. C.; Messina, L. C.; Slaughter, L. S.; Kamperman, M.; Zhou, Q.; Gruner, S. M.; DiSalvo, F. J.; Wiesner, U. Science 2008, 320, 1748-1752.

[3] (a) Yamauchi, Y. J. Ceram. Soc. Jpn. 2013, 121, 831-840. (b) Yamauchi, Y.; Suzuki, N.; Radhakrishnan, L.; Wang, L. Chem Rec. 2009, 9, 321-339.

[4] Wang, H.; Jeong, H. Y.; Imura, M.; Wang, L.; Radhakrishnan, L.; Fujita, N.; Castle, T.; Terasaki, O.; Yamauchi, Y. J. Am. Chem. Soc. 2011, 133, 14526-14529.

[5] Choi, K. S.; McFarland, E. W.; Stucky, G. D. Adv. Mater. 2003, 15, 2018-2021.

[6] (a) Attard, G. S.; Bartlett, P. N.; Coleman, N. R. B.; Elliott, J. M.; Owen, J. R.; Wang, J. H. Science 1997, 278, 838-840; (b) Kijima, T.; Yoshimura, T.; Uota, M.; Ikeda, T.; Fujikawa, D.; Mouri, S.; Uoyama, S. Angew. Chem. Int. Ed. 2004, 43, 228-232.

[7] (a) Shui, J. I.; Chen, C.; Li, J. C. M. Adv. Funct. Mater. 2011, 21, 3357-3362; (b) Tominaka, S.; Hayashi, T.; Nakamura, Y.; Osaka, T. J. Mater. Chem. 2010, 20, 7175-7182.

[8] (a) Zhang, W.; Yang, J.; Lu, X. ACS Nano 2012, 6, 7397-7405; (b) Bi, Y.; Ye, J. Chem. Commun. 2010, 46, 1532-1534.

[9] (a) Wang, H.; Wang, L.; Sato, T.; Sakamoto, Y.; Tominaka, S.; Miyasaka, K.; Miyamoto, N.; Nemoto, Y.; Terasaki, O.; Yamauchi, Y. Chem. Mater. 2012, 24, 1591-1598; (b) Li, C.; Sato, T.; Yamauchi, Y. Angew. Chem. Int. Ed. 2013, 52, 8050-8053; (c) Ataee-Esfahani, H.; Liu, J.; Hu, M.; Miyamoto, N.; Tominaka, S.; Wu, K. C. W.; Yamauchi, Y. Small 2013, 9, 1047-1051; (d) Li, C.; Wang, H.; Yamauchi, Y. Chem. Eur. J. 2013, 19, 2242-2246.

[10] Wang, L.; Nemoto, Y.; Yamauchi, Y. J. Am. Chem. Soc. 2011, 133, 9674-9677.

[11] (a) Huang, X.; Zhu, E.; Chen, Y.; Li, Y.; Chiu, C. Y.; Xu, Y.; Lin, Z.; Duan, X.; Huang, Y. Adv. Mater. 2013, 25, 2974-2979; (b) Huang, X.; Zhang, H.; Guo, C.; Zhou, Z.; Zheng, N. Angew. Chem. Int. Ed. 2009, 48, 4808-4812; (c) Zhang, Y.; Janyasupab, M.; Liu, C. W.; Li, X.; Xu, J.; Liu, C. C. Adv. Funct. Mater. 2012, 22, 3570-3575; (d) Guo, S.; Dong, S.; Wang, E.; Chem. Commun. 2010, 46, 1869-1871.

[12] Wang, L.; Yamauchi, Y. Chem. Eur. J. 2011, 17, 8810-8815.

[13] Mohan, Y. M.; Premkumar, T.; Lee, K.; Geckeler, K. E. Macromolecular Rapid Commun. 2006, 27, 1346–1354.

Graphical abstract

A Universal Approach to Preparation of Colloidal Mesoporous Platinum Nanoparticles with Controlled Particle Size in a Wide Range from 20 nm to 200 nm

Cuiling Li,[a] Masataka Imura,[a] and Yusuke Yamauchi[a,b,c]*

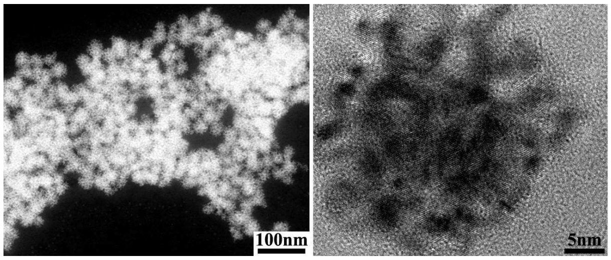

We report a universal method for preparation of mesoporous Pt nanoparticles with tunable particle sizes by changing the surfactant concentration.